# Supporting Information

**Supporting Information Text S1.**

**Sequence Design**

The CEST saturation block, placed before a metabolite cycled semi-LASER spectroscopy localization sequence, consists of a train of Gaussian pulses and alternating spoiler gradients in-between the pulses for crushing undesired transversal magnetization (1),(2). The amplitude of the last spoiler gradient is increased to ensure complete dephasing of transverse magnetization. A train of pulses is often used in CEST sequences rather than continuous–wave saturation, as the latter is limited by specific absorption rate restrictions or hardware constraints. For a train of pulses, the average $B_1$ can be calculated (1).

$$\boldsymbol{B_{1,avg}} = \sqrt{\frac{1}{\tau_{sat}} \int_0^{\tau_{sat}} \boldsymbol{B_1^2 dt}} \quad \textbf{[S1]}$$

$$= \sqrt{\frac{p_2}{\eta}} * \frac{\pi * \alpha}{180° * \gamma * p_1 * \frac{\tau_{sat}}{n}} \quad \textbf{[S2]}$$

The factors $p_1$ and $p_2$ describe the ratio of the average amplitude to the maximum amplitude and the ratio of the average of the square of the amplitude to the square of the maximum amplitude of the Gaussian saturation pulse, respectively. In this study this yielded $p_1$= 0.69 and $p_2$= 0.57 for the standard Siemens Gaussian pulse[1]. The average strength of $B_1$ is further defined by the flip angle $\alpha$ and the total length of the saturation block $\tau_{Sat}$. $\eta$ describes the duty cycle of the saturation:

$$\boldsymbol{\eta} = \frac{n * \tau_{pulse\_dur}}{\tau_{Sat}} \quad \textbf{[S3]}$$

The offset frequency $\Delta_{ppm}$, at which the saturation pulses are applied, was varied linearly in each measurement to cover the desired ppm range. For a fixed frequency range to be covered, the number of measurements determined the sampling distance between offset values. For the first measurement the saturation was placed very far outside the observed frequency range (at -100 ppm). This measurement is referred to as $M_0$ and was used for normalization and reference for the evaluation of saturation effects.

[1] Note that the gyromagnetic ratio $\gamma$ is given in $\frac{rad}{s*T}$

**Supporting Information Text S2.**

**Fitting procedure**

Metabolite basis sets were simulated in VESPA (3) for the specific semiLASER sequence for the given echo time including timing and RF pulse shapes, but neglecting off-resonance terms from slice selection gradients. 18 metabolites were included in the fitting model[2]: Aspartate; Creatine (Cr); γ-aminobutyric-acid; Glucose (Glc); Glutamine (Gln); Glutamate (Glu); Glycine; Glycerophosphorylcholine (GPC); Glutathione; Lactate (Lac); myo-Inositol (mI); N-acetylaspartate (NAA); N-acetylaspartylglutamate (NAAG); Phosphocholine (PCho); Phosphocreatine (PCr); Phosphorylethanolamine; scyllo-Inositol; Taurine. The MM background (MMBG) was modeled with 64 equally spaced Voigt lines (spaced by 0.05 ppm) between 0.7 and 4.1 ppm each with a Gaussian broadening of 5 Hz and a Lorentzian broadening of 9 Hz. The fitting range was limited to 0 – 4.1 ppm. The metabolite fit model was simplified by assuming identical phase, frequency offset and broadening parameters for all metabolites in all spectra.

For better convergence and consistency between spectra, the fitting procedure was divided into four subsequent steps:

1. Areas, offset, phase, Lorentzian and Gaussian broadening parameters fitted using the $M_0$ spectrum to obtain starting values for subsequent fit of the CEST MR spectra.
2. Sequential fit of metabolite and MMBG areas for all spectra using the offset, phase, Lorentzian and Gaussian broadening parameters from step 1.
3. Fit of offset, phase and broadening parameters using all spectra simultaneously, but keeping the amplitudes as found in step 2.
4. Repetition of step 2, now with the adapted parameters from step 3.

[2] In the results, we mostly cannot distinguish between some of the strongly overlapping metabolites and thus will use $Cr_{tot}$ for Cr + PCr, $Cho_{tot}$ for GPC + PCho, and $NAA_{tot}$ for NAA + NAAG. The same notation is used to refer to the prominent singlets in the spectrum

**Supporting Information Text S3.**

**Influence of relaxation times on direct saturation model**

For continuous-wave irradiation, the full-width half-maximum (FWHM) of the Lorentzian curve describing direct saturation can be described as function of $B_1$ amplitude and the ratio between $T_1$ and $T_2$ values of the irradiated resonance line (2):

$$FWHM = \frac{\gamma * B_1}{\pi} * \sqrt{\frac{T_1}{T_2}} \quad [S4]$$

with the gyromagnetic ratio $\gamma$ in $\frac{rad}{s*T}$.

The fact that this equation suggests metabolite-specific FWHM was used to approximate the direct saturation effects for resonances close to water based on the fitted data for N-acetylaspartate (NAA) at all three $B_1$ and the fitted data for NAA and $Cho_{tot}$ (Glycerophosphorylcholine + Phosphocholine) at the lowest $B_1$. Since pulsed, rather than continuous-wave, irradiation was applied the derivation of these FWHM did not rely on proportionality between $B_1^{eff}$ and FWHM, but rather on the measured FWHM of NAA at all $B_1$s.

**Direct saturation correction method**

For the construction of a direct saturation correction method, it was considered easiest to evaluate the saturation effect as a function of irradiation frequency for the three main singlet resonances in the spectrum. However, with standard linear combination fitting using metabolite basis sets that include the resonances of whole metabolite spectra, the fitting results for these singlets are not only affected when they are reduced in intensity through saturation directly, but also when another part of the spectrum for the pertinent metabolite is influenced by the irradiation. Hence, spectra were refitted with a fitting model that was modified to allow adaptation of the area parameters of the main singlets in the spectra (methyl groups of $Cr_{tot}$, NAA and $Cho_{tot}$) independently of the area values for the resonances for the rest of those molecules.

Considering that the width of the direct saturation effect depends on $B_{1,avg}$ and that MT effects from water saturation are expected, different numbers of spectra were used for the definition of the direct saturation effect, which depended on $B_1$ and the resonance frequency of the singlet peak. For the lowest $B_1$ of 0.4 µT, the fits of all singlets as function of saturation offsets between -6.0 and -0.9 ppm (spectroscopic ppm range of -1.3 to 3.8 ppm) were used to describe the direct saturation as a single Lorentzian line in the constructed z-spectrum. For higher $B_1$, this Lorentzian was only

constructed for the NAA singlet, and the response for the other singlets was estimated assuming constant ratios with respect to NAA (see the paragraph on the theoretical dependence of the width of the direct saturation on relaxation times). The spectra including a theoretical direct saturation effect $Spec_{n,direct_{sat}}$ were then calculated by multiplying the measured $M_0$ spectrum $Spec_{M0,measured}$ with the saturation function based on the Lorentzian saturation model $Lorentzian_{n,direct\ sat}$.

$$Spec_{n,direct_{sat}} = Spec_{M0,measured} * (1 - Lorentzian_{\omega_{sat},direct\ sat}) \quad \textbf{[S5]}$$

Two cases were constructed. First, addressing MT for the creatines, using the model for direct creatine saturation. Second, aiming at MT on all other metabolites, using the averaged saturation effects for NAA and GPC (Lorentzian with a width calculated as the average of the full width at half maximum (FWHM) of NAA and $Cho_{tot}$). The whole procedure is illustrated in Supporting Information Figure S1.

**Supporting Information Figure S1. Illustration of the calculation of the direct saturation correction for the metabolite spectra.**

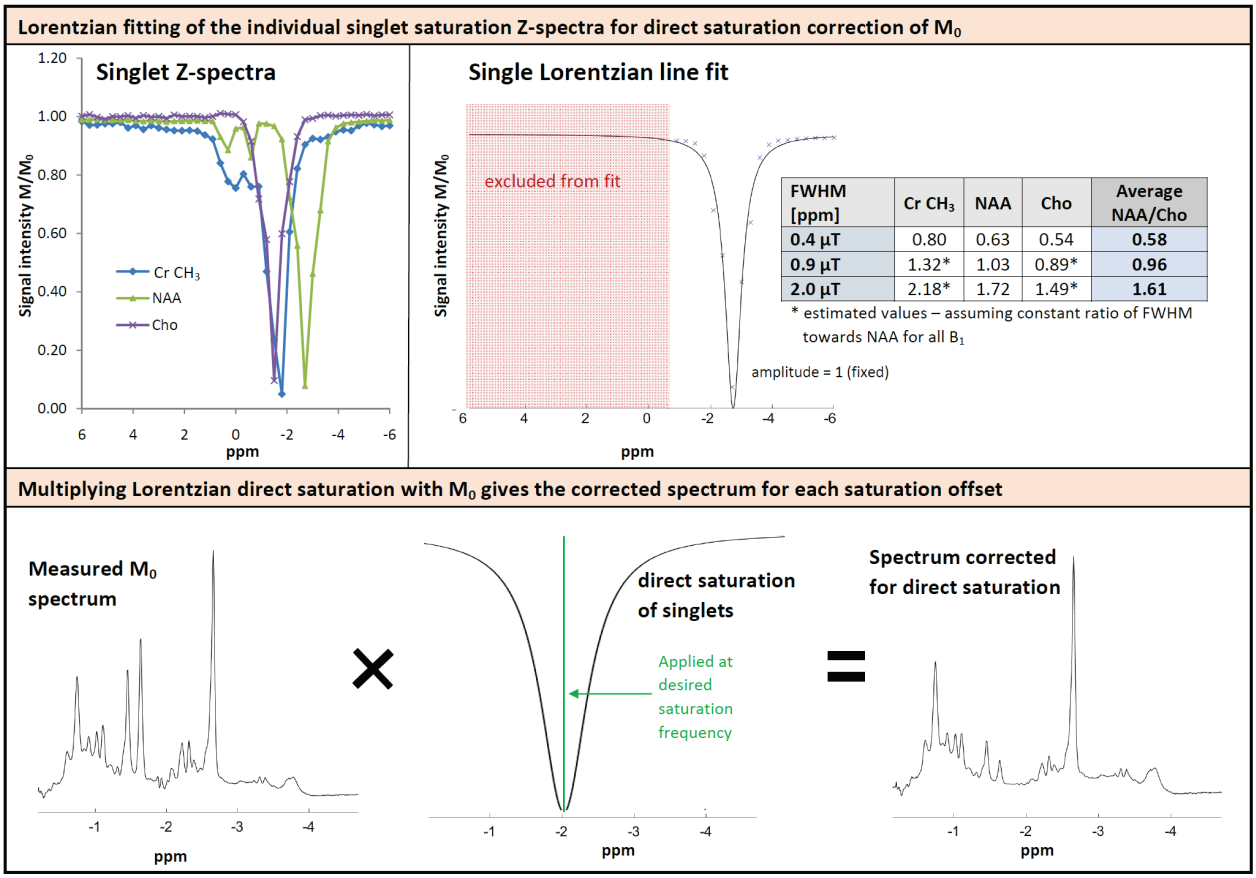


***Figure S1*** *– Illustration of the calculation of the direct saturation correction for the metabolite spectra. Upper part: Signal intensity was fitted in FiTAID for the three individual singlets (left) and fitted with a single Lorentzian line in MATLAB (right). For $B_1$ = 0.4 µT all were fitted. For higher $B_1$, only NAA was fitted to avoid interference with ST effects at the water resonance. The remaining metabolite FHWMs were estimated, assuming a constant ratio with respect to NAA for all $B_1$. The resulting values from both the fitting and the estimation process are listed in the table besides the Lorentzian fit. FWHM values of Cr $CH_3$ as well as the average of Cho and NAA singlets were then used to calculate the Lorentzian direct saturation of the spectra. Lower part: Multiplying the $M_0$ spectrum with the direct saturation effect applied at the desired frequency offset gives the $M_0$ spectrum corrected for direct saturation.*

**Supporting Information Text S4**

**Fitting z-spectra**

For the calculation of the water z-spectrum, the intensity of the water signal $M(\omega)$ was calculated from the magnitude of the second data point of the water signal FID[3] for each saturation frequency $\Delta_{ppm}$ and divided by the water intensity from $M_0$.

Each pool $n$ is represented by a Lorentzian line with three fitting parameters: the offset from the water frequency $\omega_{0,n}$, the amplitude $a_n$ and the FWHM $\Gamma_n$. The following MT effects were included: exchange pools of amides, amines and the hydroxyl groups, as well as an upfield NOE. In addition, the model includes direct water saturation and a general broad MT effect, summing up to a total of 6 pools. Furthermore, a factor $Z_{base}$ corrects for an unspecific reduction of the signal (4). Thus, the measured data $M(\omega)$ is modeled as $S(\omega)$

$$S(\omega) = Z_{base} - \sum_{n=1}^{6} L_n \quad \text{[S6]}$$

with

$$L_n = a_n * \frac{1}{1+4*\left(\frac{\omega-\omega_{0,n}}{\Gamma_n}\right)^2} \quad \text{[S7]}$$

For the fit in MATLAB using least squares estimation, parameter values were restricted to physically meaningful ranges mostly based on Ref (4) and listed below. The offset for direct water saturation, $\omega_{0,n}$ was restricted to a narrower range of ±0.2 ppm, given the maximal drift found in the observed spectra. The same range was chosen for the hydroxyl group around 0.9 ppm (5), which was assumed to have the same range for the width as the amine groups:

- $\omega_{0,direct\ water\ saturation}$ [-0.2 - 0.2 ppm], $\Gamma_{direct\ water\ saturation}$ [0.3 – 10 ppm]
- $\omega_{0,amides}$ [3 – 4 ppm], $\Gamma_{amides}$[0.4 – 3 ppm]
- $\omega_{0,amines}$ [1 – 2.5 ppm], $\Gamma_{amines}$[1 – 3.5 ppm]
- $\omega_{0,hydroxyl}$ [0.7 – 1.1 ppm], $\Gamma_{hydroxyl}$[1 – 3.5 ppm]
- $\omega_{0,NOE}$ [ -3 – -4 ppm], $\Gamma_{NOE}$[1 – 5 ppm]

The general MT effect was fixed in offset to $\omega_{0,MT}$ = -2.3 ppm (6) and width to $\Gamma_{MT} = 55$ ppm (average value of proposed range from 10 - 100 ppm).

[3] The first point in the FID that corresponds to the peak area is not well suited because it is influenced by receive filters

**Supporting Information Figure S2. Illustration of fitted spectra**

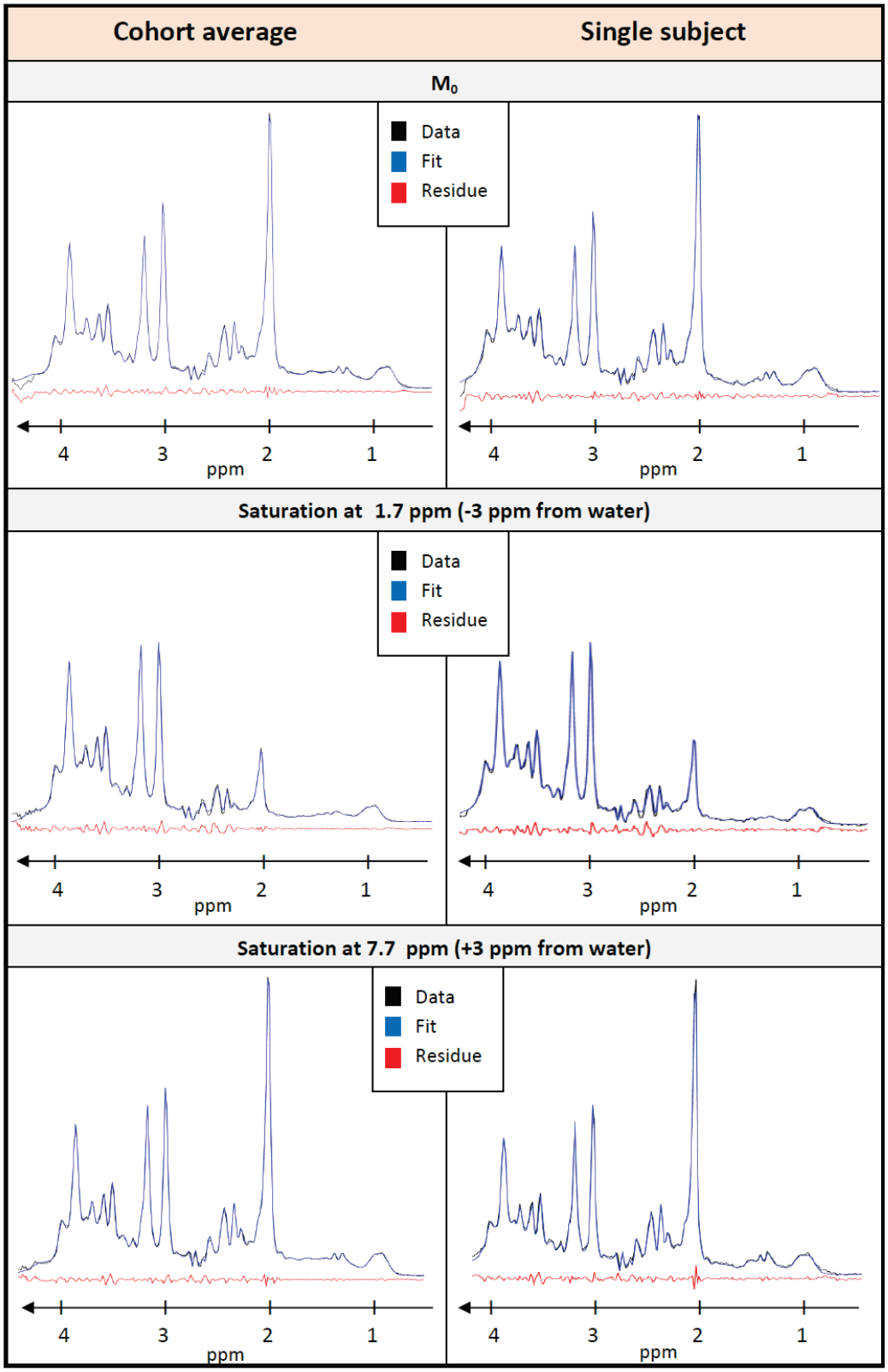


***Figure S2*** *– Illustration of fitting results for the metabolite spectra of the cohort average (left) and a single subject (right) for saturation with 0.9 µT for different saturation frequencies. Fitting residues displayed in red. Fitting performance was good in all cases, systematic bias at NAA singlet and mI probably caused by small frequency shifts from the assumed Literature resonances. Residues in coupled metabolites under saturation are probably caused by the fixed area relations of the individual patterns.*

**References in supporting information**


1. Zu Z, Li K, Janve VA, Does MD, Gochberg DF. Optimizing pulsed-chemical exchange saturation transfer (CEST) imaging sequences. Magn Reson Med. 2012;66:1100–1108.

2. Sun PZ, Wang E, Cheung JS, Zhang X, Benner T, Sorensen AG. Simulation and optimization of pulsed radio frequency irradiation scheme for chemical exchange saturation transfer (CEST) MRI — demonstration of pH-weighted pulsed-amide proton CEST MRI in an animal model of acute cerebral ischemia. Magn Reson Med. 2011;66:1042–1048.

3. Soher BJ, Semanchuk P, Todd D, Steinberg J, Young K. VeSPA: Integrated applications for RF pulse design, spectral simulation and MRS data analysis. In: *Proceedings of the 19th Annual Meeting of ISMRM, Montreal, Canada, 2011. p. 1410*.

4. Windschuh J, Zaiss M, Meissner J, et al. Correction of B1-inhomogeneities for relaxation-compensated CEST imaging at 7T. NMR Biomed. 2015;28:529–537.

5. van Zijl PCM, Lam WW, Xu J, Knutsson L, Staniszc GJ. Magnetization transfer contrast and chemical exchange saturation transfer MRI. Features and analysis of the field- dependent saturation spectrum. Neuroimage. 2018;168:222–241.

6. Hua J, Jonesa CK, Blakeleyd J, Smith SA, Zijl PCM van, Zhou J. Quantitative description of the asymmetry in magnetization transfer effects around the water resonance in the human brain. Magn Reson Med. 2007;58:786–793.